Lawrence Berkeley National Laboratory

Title
Supplementary material to "Induced seismicity risk analysis of the hydraulic stimulation of a geothermal well on Geldinganes, Iceland"

Permalink

Authors
Broccardo, Marco
Mignan, Arnaud
Grigoli, Francesco
et al.

Publication Date

DOI

Peer reviewed

Natural Hazards
and Earth System
Sciences

Open Access

EGU

Supplement of

Induced seismicity risk analysis of the hydraulic stimulation of a geothermal well on Geldinganes, Iceland

Marco Broccardo et al.

Correspondence to: Marco Broccardo (bromarco@ethz.ch)

Supplements

S1 GMPEs GMICE and Scenario based intensity

In this Supplementary material, we first show the trellis plots of the GMPE Figure S1 and of the GMPE&GMICE combination, Figure S2. The GMICE coefficients are reported in Table S1.
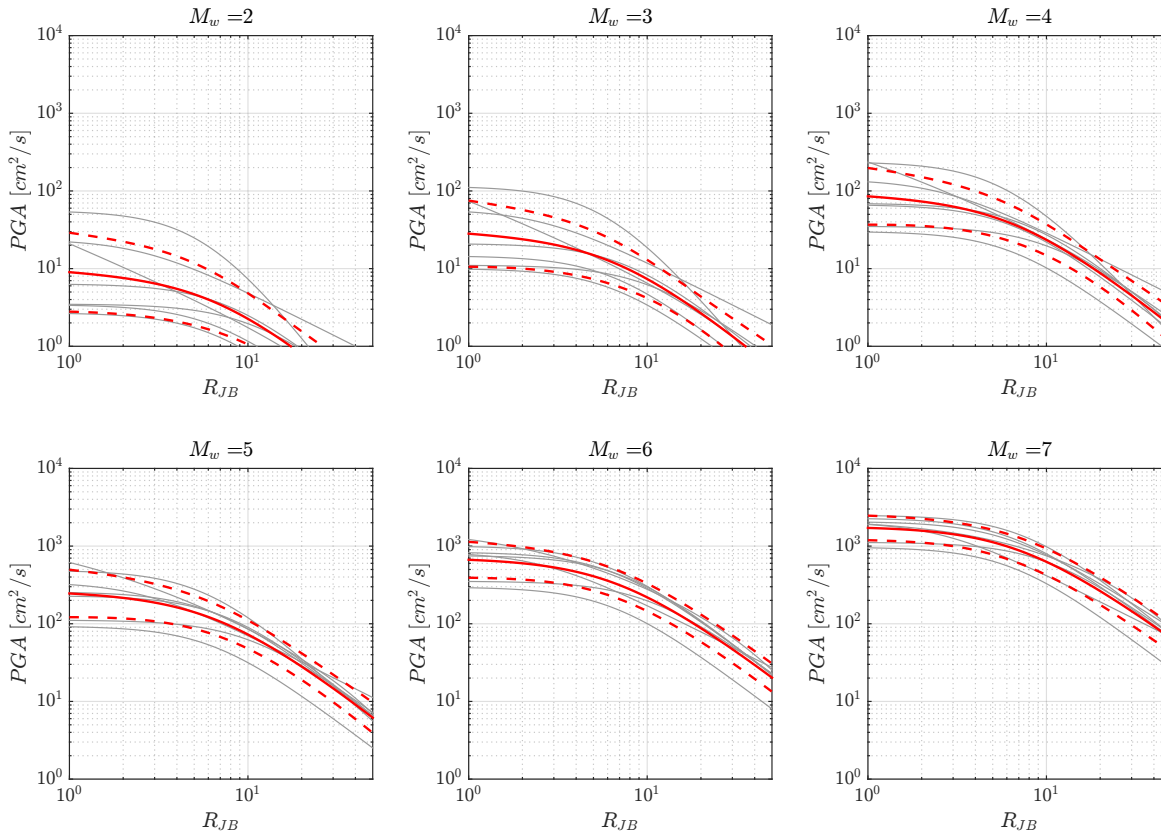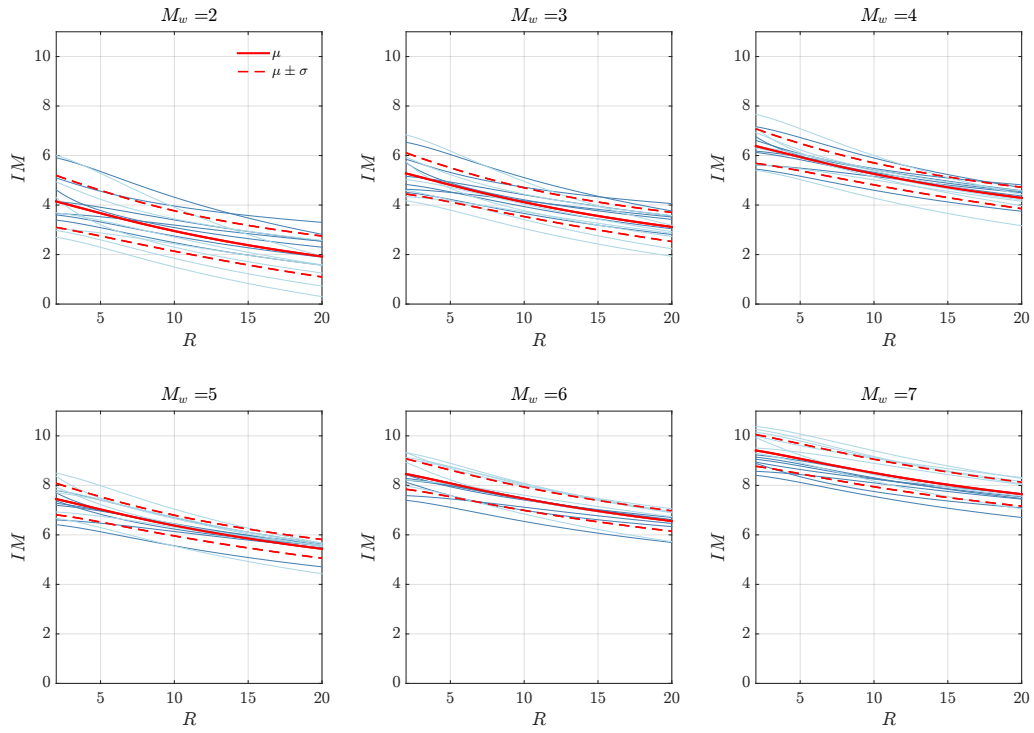
5

Figure S1. Trellis Plots for the selected GMPEs models. Following the same representation of Rupakhety and Sigjörnsson (2009), solid red lines are the epistemic mean and the dash lines the epistemic mean plus minus the epistemic standard deviation (in log scale).

Figure S2 GMICE model. Solid red lines are the epistemic mean and the dash lines the epistemic mean plus minus the epistemic standard deviation.

Table S1: GMICE parameter list

	$\mu_{IM}(PGA)$	σ_{GMICE}		σ_{GMPE}	a	σ_{TOT}
Faccioli and Cauzzi (2006) Units: [m/s]	$1.96\log_{10}(PGA)+6.54$	0.89	1-AB10	0.175	1.96	0.954
			2-CF08	0.176	1.96	0.955
			3-Zh06	0.391	1.96/ln(10)	0.950
			4-Am05	0.175	1.96	0.954
			5-DT07	0.177	1.96	0.955
			6-GK02	0.403	1.96/ln(10)	0.954
			7-RS09	0.287	1.96	1.053
Faenza and Michelini (2010) Units: [cm/s]	$2.58\log_{10}(PGA)+1.68$	0.35	1-AB10	0.175	2.58	0.571
			2-CF08	0.176	2.58	0.573
			3-Zh06	0.391	2.58/ln(10)	0.560
			4-Am05	0.175	2.58	0.571
			5-DT07	0.177	2.58	0.575
			6-GK02	0.403	2.58/ln(10)	0.571
			7-RS09	0.287	2.58	0.819

2

Given the very large epistemic uncertainty governing the parameter a_{fb} and b of the seismogenic source model, here we propose a conditional probability distribution of PGA and IM: i.e., $P(PGA > pga|M = m, r)$ (also known as scenario based distribution). Figure S3 shows the scenario-based distributions for both PGA and IM.
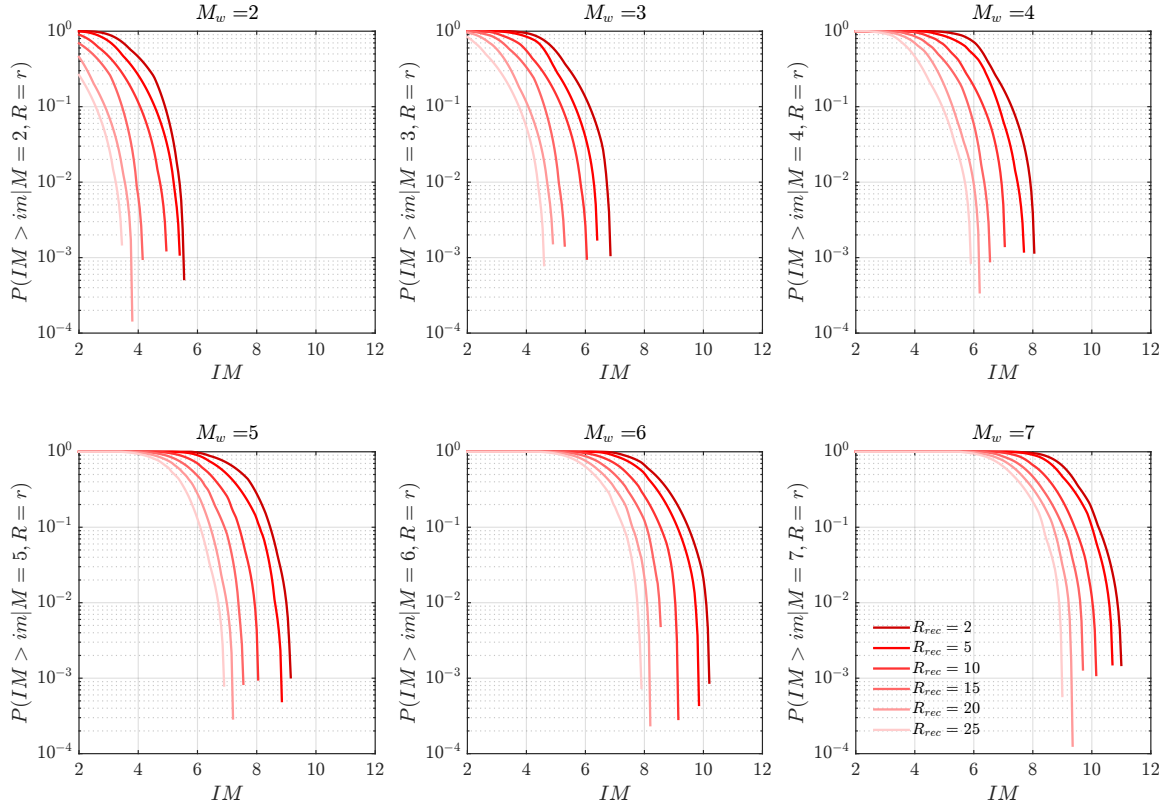
20

Figure S3 Collection of epistemic medians of $P(IM > im|M = m, R = r)$ for different Magnitude and site to source distances

S2 Exposure, population and assets

The exposed area to the introduced anthropogenic hazard is defined by the building stock within approximately 20 km from
25 the injection point. The region is identified with the so-called Höfuðborgarsvæðiðm (i.e., the capital region, which includes the capital Reykjavík and six municipalities). This is the largest and densest urban agglomeration in the country with a population of 229,000, which corresponds to circa 65% of the total Icelandic population.

For this study, detailed and precise information of the Reykjavik building stock and population exposed is not readily available and hence not used. Therefore, this description is limited to a macro analysis based on the work of Bessason and

30 Bjarnason (2016), the Icelandic Property Registry, and the European Seismic Risk service. Based on the Icelandic Property Registry and on Bessason and Bjarnason (2016), it is possible to categorize the building stock by the class of buildings. According to Bessason and Bjarnason (2016), the vast majority of residential buildings (reinforced concrete, timber and pumice block buildings) have shear walls as a lateral structural system against seismic forces. Buildings made of hollow pumice represent a small percentage and can be considered according to Bessason and Bjarnason (2016) as masonry buildings. No

35 information is available at the present time on soil conditions at construction sites, which is assumed to be in firm soil condition. We finally highlight that these evaluations are a first-order estimate only. Given the current lack of a detailed exposure model, we do not include in the present study any aggregate monetary loss analysis.

In addition, according to the European Seismic Risk service, the residential building stock of Iceland is composed of circa 70,000 buildings with a total of 68,000 million Euro of replacement costs. In a first-order inference of the number of

40 residential buildings, we can estimate that there are circa 55-65% of the total amount, a percentage a bit lower than the population proportion. This assumes that in urban areas, the number of persons per building is higher. Given that, a crude estimate of the number of residential buildings in the considered area is given by a range of 38,500-45,500 units for a total replacement cost of [37,400-44,200] millions of euro.

We highlight that these evaluations are a crude first-order estimate only. Given the current lack of a detailed exposure

45 model, we do not include in the present study an aggregate monetary loss analysis (since it will introduce an additional level of deep uncertainty). However, we introduced a low damage threshold risk metric to measure and prevent the likelihood of large damage in the building stock.

50

S3 Scenario Based *IR*, and *DR*

In this section, we first present the scenario *IR* for different magnitudes, locations and building typologies. The scenarios are derived by using the mean of the GMICE and converted into *IR* by using the vulnerability model (Lagomarsino and Giovinazzi, 2006, and modified by Mignan et al. 2015, Figure S4, Table S2) and the conditional probability of fatalities for a

55 given damage grade (Galanis et al. 2018, Hazus MH MR3, 2003). Figure S5 shows the *IR* scenario-based calculations. We can conclude that for a magnitude lower than 4 the $IR = q_{IR,.5} \leq 10^{-6}$ is satisfied for all the building classes.
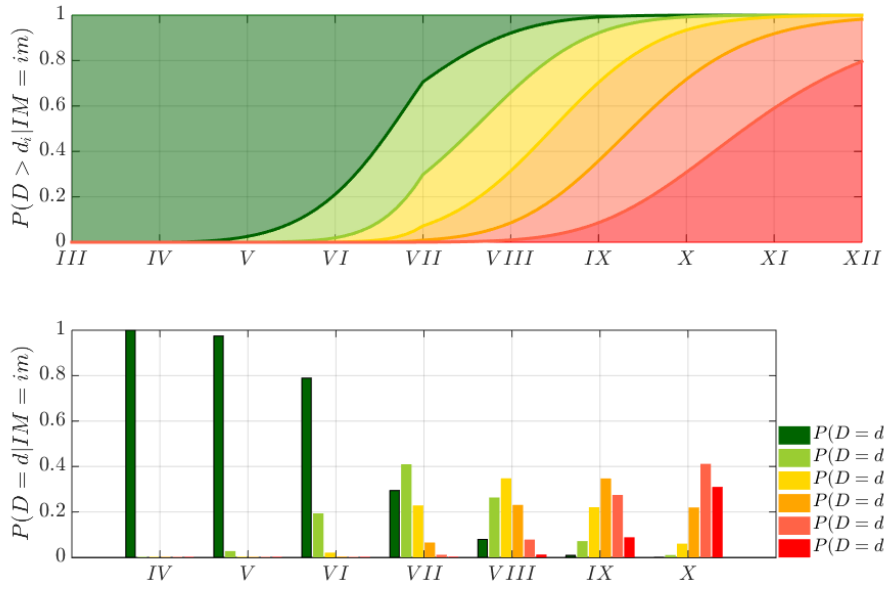
4

Figure S4 Top subplot: fragility functions, $P(D > d_k | IM = im)$, bottom subplot: probability mass function $p_D(d_k)$ for different level of intensity. The discontinuity at $im = VII$ is introduced by Mignan et al. (2015).
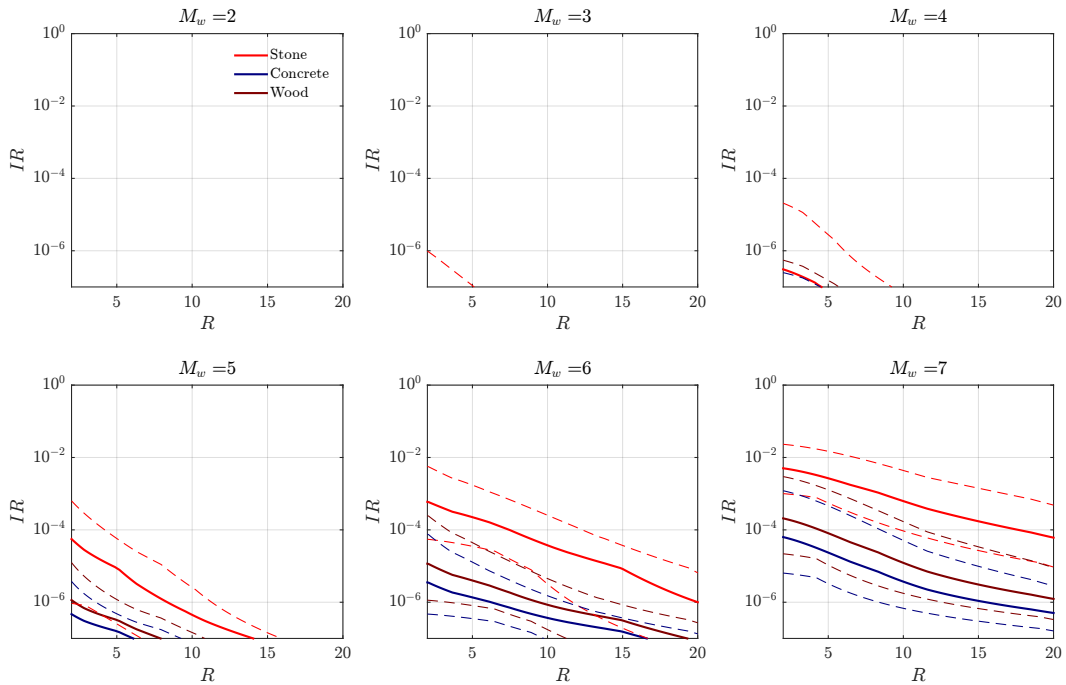
60

Figure S5. Individual Risk for different magnitude, distance and typology of buildings.

Further, we present damage-based scenarios derived by using the mean of the GMICE converted into DR by using the local fragility functions proposed by Bessason, B. and Bjarnason, 2016, reproduced in Figure S6.
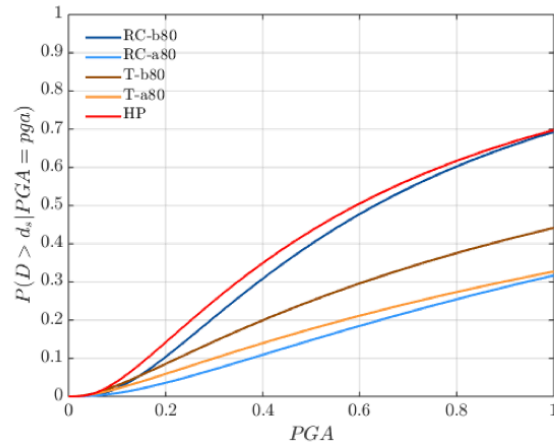

Figure S6 Fragility function for low damage estimation

Figure S7 shows the damage scenario for a magnitude 3 and 4, which represent the scenario limit for observing $DR \leq 10^{-2}$.
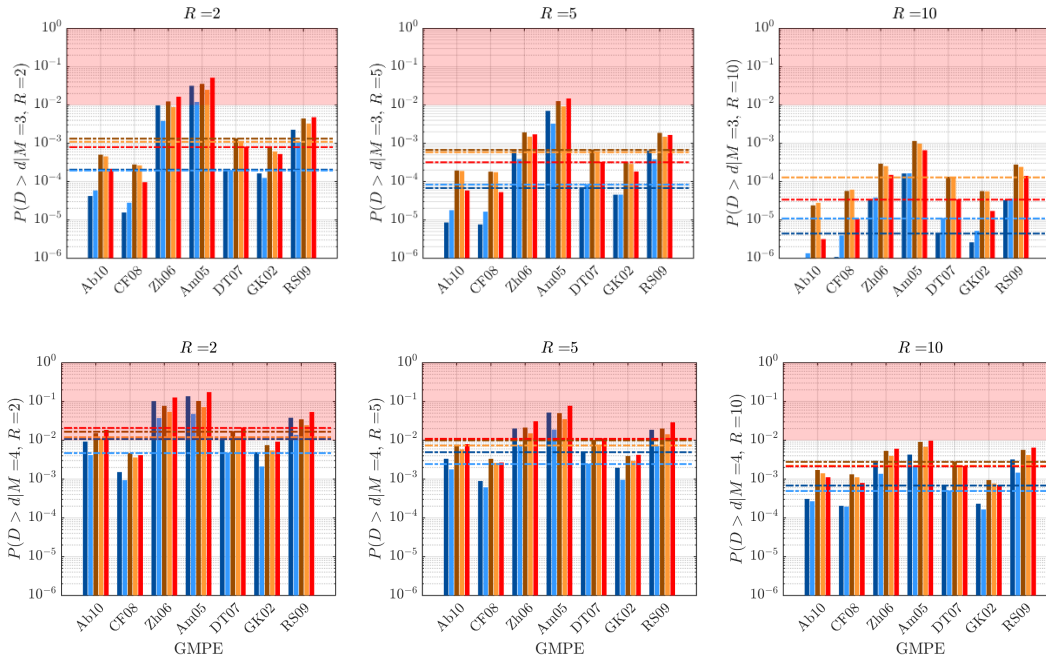

Figure S7. Scenario-based Damage Risk for magnitude 3 (first 3 subplots) or 4 (second 3 subplots). Dashed lines represent the median for each building class.

Table S2 Vulnerability index per building class. $V^0 V^+, V^-$ & V^{--}, V^{++} values are based on Mignan et al. (2015). Bolt fonts indicate the selected model.

Building class	Class description	V^{--}	V^-	V^0	V^+	V^{++}

Masonry (M)	M1	Simple stone with timber slabs	0.460	0.650	0.740	0.830	1.020
	M2	Massive stone with timber slabs	0.300	0.490	0.616	0.793	0.860
	M3	Brick with concrete slabs	0.300	0.490	0.616	0.793	0.860
	M4	Simple stone with hollow-core slabs	0.420	0.610	0.700	0.790	0.900
	M5	**Brick with hollow-core slabs**	0.320	**0.500**	0.650	0.800	0.870
	M6	Massive stone with hollow-core slabs	0.320	0.500	0.650	0.800	0.870
	M7	Brick with timber slabs	0.460	0.650	0.740	0.830	1.020
Reinforced concrete	RC 1	Concrete moment frames	0.140	0.207	0.442	0.640	0.860
	RC 2	**Concrete shear walls**	0.140	0.210	**0.386**	0.510	0.700
	RC 3	Concrete walls and brick masonry walls	0.150	0.220	0.400	0.520	0.710
	RC 4	Hennebique system	0.250	0.300	0.500	0.700	0.850
	RC 4	Concrete moment frames with infills	0.150	0.220	0.402	0.520	0.710
Steel	S1	Steel Structures (moment & brace F)	-0.020	0.170	0.325	0.480	0.700
	S2	Old steel structures	0.150	0.220	0.400	0.520	0.710
Wood	**W1**	**Timber structures**	0.140	0.207	**0.447**	0.640	0.860
	W2	Half-timbered structures	0.170	0.240	0.480	0.670	0.890

S4 Sensitivity analysis details

In this section, we present the details of the modified version of the Morris method for sensitivity analysis. The modified version is a global sensitivity measure which accounts for all possible base rate model. To obtain a global sensitivity measure, we first define the local sensitivity measure of the parameter i with respect to the model base j as

$$d_i(j) = \frac{\max[\text{QoI}_i(j)] - \min[\text{QoI}_i(j)]}{\Delta},$$
(S1)

where $\max(\text{QoI}_i(j))$ and $\min(\text{QoI}_i(j))$ are the maximum positive and negative swings of the selected QoI obtained by holding all the parameter different from i fixed to their base value j. Moreover, $\Delta = \max(\text{QoI}) - \min(\text{QoI})$ is the global maximum swing of the QoI (which is by definition independent on i or j). Then, we define two global sensitivity measures as

$$\mu_{d_i} = \frac{1}{J} \sum_{j=1}^{J} d_i(j),$$

(S2)

$$\bar{d}_i = \max[d_i(j)].$$

(S3)

In particular, the sensitivity measure μ_{d_i} aims to provide an average relative contribution of the parameter i over all possible base models. On the other hand, the sensitivity measure $\bar{d}_i$, aims to describe the maximum contribution of the parameter i over all possible base models. Observe that $0 \leq \mu_{d_i} \leq 1$ and $0 \leq \bar{d}_i \leq 1$ and the sum over i for both, in general, is not equal to 1

90 (obviously one can normalize the output if this is a desired property). Therefore, the following sensitivity method shall be used only to rank the input uncertainties and to understand their relative contribution and not the absolute contribution.

In this study IR and DR, range from medium-low probability values to very low probability values, with values that go from 10^{-2} (DR) up to 10^{-14} (IR). Therefore, to avoid the dominant contribution of the branches with higher probability content, we performed a log transformation. It follows that the two QoIs are: $\log(IR)$ and $\log(DR)$. In the following we report the results

95 for $\bar{d}_i$ (while μ_{d_i} are reported in the main text). Figures S8 and S9 show the same trend observed for μ_{d_i} with the rate model dominant for both datasets and with a relatively larger contribution of the dataset based on Table 3.1.
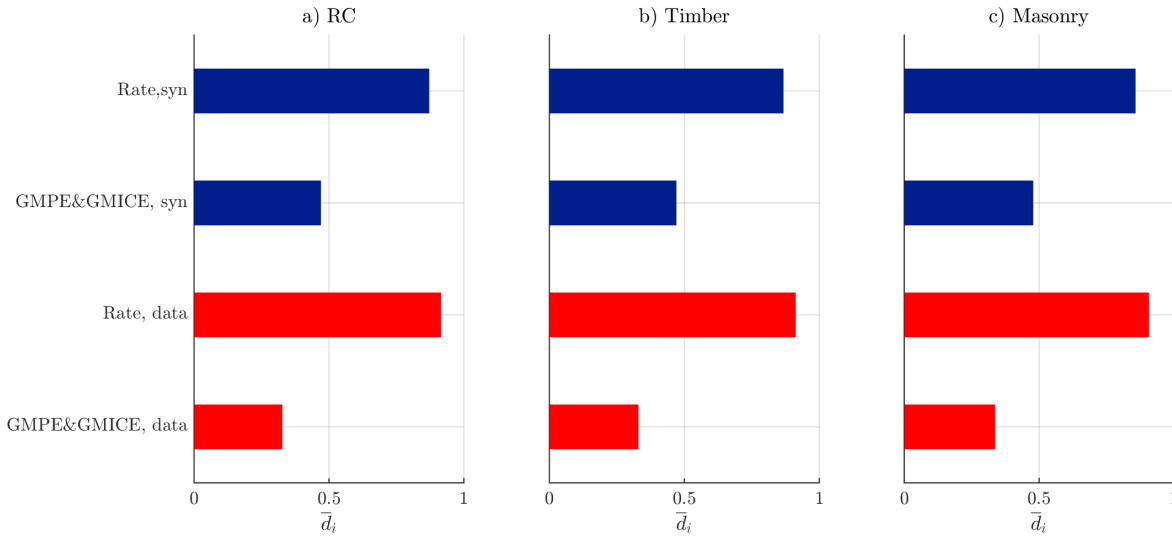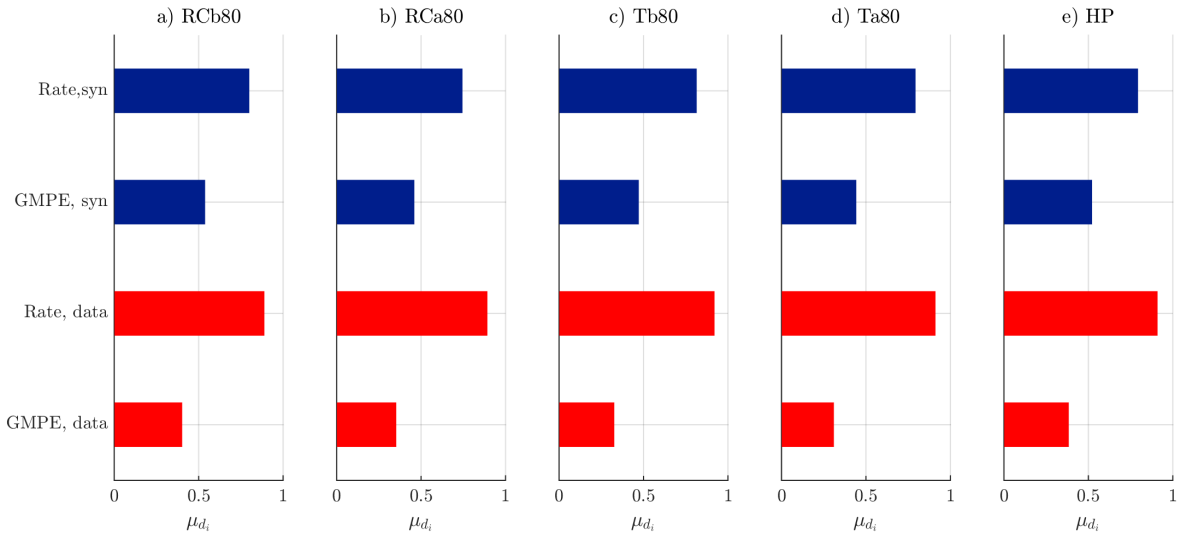
100

Figure S8. Sensitivity analysis of IR (observe that the QoI is $\log IR$) based on the sensitivity measure $\bar{d}_i$ for each building class

a) RCb80 b) RCa80 c) Tb80 d) Ta80 e) HP

105

Figure S9. Sensitivity analysis of DR (observe that the QoI is $\log DR$) based on the sensitivity measure $\overline{d_i}$ for each building class

9